The spin evolution of accreting and radio pulsars in binary systems

Nielsen, A.B.

CHAPTER 3

Coherent variability of GX 1+4

The accreting pulsar GX 1+4 is a symbiotic X-ray binary system with a M-type giant star companion. The system has a spin period of about 150 s and a proposed strong magnetic field of 10^{12}–10^{14} G. In this chapter we study the coherent variability of the source and attempt to find a phase-coherent solution for the pulsar. We also test for the presence of a pulse phase - flux correlation, similar to what is observed for the accreting millisecond X-ray pulsars, in order to test whether this feature is dependent on the magnetic field strength. We find that no phase coherent solution exists which suggests that the pulsar is accreting plasma from a wind rather than an accretion disc. We also find evidence that the pulse phase is not correlated with the X-ray flux, which strengthens the idea that such relation might be present only in weak magnetic field sources like accreting millisecond pulsars.

A. Bak Nielsen & A. Patruno
Paper submitted to MNRAS, 2018

3.1 Introduction

The X-ray pulsar GX 1+4 was first discovered in 1970 by balloon X-ray observations at energies above 15 keV by Lewin et al. (1971). GX 1+4 is the first discovered accreting pulsar in a low mass symbiotic X-ray binary system (SyXB) and it is unique among the symbiotic binaries, due to the primary star being a neutron star and not a white dwarf or a main sequence star (Davidsen et al. 1977; Hinkle et al. 2006; Serim et al. 2017). The companion of GX 1+4 is V2116 Oph (Chakrabarty et al. 1997), which is an M giant star, of about $1.2 M_{\odot}$ and the pulsar is thought to have a mass of $1.35\,M_{\odot}$ (González-Galán et al. 2012). The M giant is probably not filling its Roche lobe, but the pulsar is instead accreting through a stellar wind (Chakrabarty et al. 1997; Hinkle et al. 2006). The orbital period of GX 1+4 was originally proposed to be 304 days (Cutler et al. 1986; Pereira et al. 1999). This value was, however, revised to be 1161 days and it remains to be confirmed (Hinkle et al. 2006). The orbit is modestly eccentric with e=0.10 (Hinkle et al. 2006). Torque reversals are observed in GX 1+4, with the first observations showing a clear neutron star spin-up (Nagase 1989) that, around 1987, when the pulsar reappeared, turned into a clear spin-down. During the spin-up phase, the pulsar had a spin frequency derivative of $\dot{\nu}$=$6.0\times10^{-12}\,\mathrm{Hz\,s^{-1}}$, whereas during spin down the pulsar had a spin frequency derivative of $\dot{\nu}$=$-3.7\times10^{-12}\,\mathrm{Hz\,s^{-1}}$ (Chakrabarty et al. 1997). The spin period was about 159.9 s in 2010 (Yoshida et al. 2017).

Rea et al. (2005) observed a possible electron cyclotron feature in the energy spectra, using *BeppoSAX*, at an energy of 32–37 keV. This would correspond to a magnetic field of about 4×10^{12} G, which is lower than earlier magnetic field estimates of order $B \sim 10^{13-14}$ G (Dotani et al. 1989; Mony et al. 1991; Cui & Smith 2004), inferred from spin-down episodes. It must be remarked, however, that the proposed identification of the cyclotron line is still unconfirmed (Rea et al. 2005).

An open question about GX 1+4, as well as other slow accreting pulsars in low mass X-ray binaries, is whether the presence of the neutron star magnetic field and its interaction with the accretion flow could lead to phenomena similar to those observed in accreting millisecond X-ray pulsars (AMXPs), which are much fainter and with lower magnetic fields (see Patruno & Watts 2012 for a review). The reason is that observing a similar phenomenology for example in the behaviour of pulsations might shed some light on how accretion flows and neutron star magnetospheres interact and clarify the exact role of the strength of the magnetic field and mass accretion rate. For example, a still unexplained correlation between the X-ray flux and the pulse phases is observed in several AMXPs (Patruno et al. 2009), contrary to what is predicted by accretion torque theory, where it is the spin frequency derivative and not the pulse phase that is expected to be correlated with the X-ray flux. Iłkiewicz et al. (2017) discussed the variability of GX 1+4, reporting large variations in the X-ray flux over several energy bands. The variations reach up to one to two orders of magnitude (Iłkiewicz et al. 2017; Serim et al. 2017). Due to these large variations in X-ray flux, we consider GX 1+4 an optimal system to test whether corresponding large variations in the pulse phases are present. Patruno et al. (2009) examined six known AMXPs based on the presence

of red timing noise in the pulse phases. They found that there was a correlation and in some cases an anti-correlation, between the flux and pulse phase. This was interpreted as due to the motion of the hot spot on the surface of the pulsar in response to mass accretion rate variations. It is currently not known whether a similar phenomenon exists in high field pulsars since the stronger magnetic field might prevent the movement of plasma on the neutron star surface. Bak Nielsen et al. (2017) and Patruno et al. (2012) found that such phase–flux correlation was not present in two moderately high field accreting pulsars, namely 2A 1822–371 and Terzan 5 X–2. Despite the lack of phase–flux correlations some timing noise was however observed in the pulse phase residuals of these systems. Furthermore the strength of their magnetic fields is only 1-2 orders of magnitude larger than what is seen in AMXPs, whereas their accretion rate is close to the Eddington limit. Therefore it remains to be verified whether higher magnetic field accreting pulsars show such correlation or not. Testing this hypothesis is very valuable for two reasons. On one hand, if the hot spot is moving on the surface then this effect must be taken into account when finding a pulsar timing solution. Second, the magnetic field of GX 1+4 is four to six orders of magnitude larger than those found in AMXPs and thus detecting (or not detecting) this phenomenon will help understand its origin.

In this chapter we examine long and short term fluctuations of the pulse time of arrivals, variations of the X-ray flux and we check whether there is any evidence for a pulse phase–flux correlation on the prototype system GX 1+4. In section 3.2 we go through the observations used, and in section 3.3 we present the results of our analysis. In section 3.4 we discuss the possible presence (or lack thereof) of a pulse phase–flux correlation, the observed short term variability of the source and we provide a physical interpretation of what is observed.

3.2 Observations

We have used data taken between March 6 to November 14, 2001 (ObsID=60060), thus using almost the same data range as Serim et al. (2017). We choose this dataset because Serim et al. (2017) claim to have phase connected the data and provide a timing solution for the source. The data was recorded with the Proportional Counter Array (PCA) which was on board of the Rossi X-ray Timing Explorer (*RXTE*). *RXTE*/PCA has five xenon/methane proportional counter units that are sensitive in the energy range of 2–60 keV (Jahoda et al. 2006). We use the event files with a resolution of 2^{-20} s (GoodXenon) for the timing analysis, and the Standard-2 data-mode, with a 16 s time resolution, to create the X-ray lightcurve. The lightcurve is created in the 2–16 keV energy range and the X-ray flux is averaged for each observation (ObsID) and normalized in Crab units (see top panel in Fig. 3.1). A detailed description of this procedure can be found in van Straaten et al. (2003). We perform the timing analysis by selecting the energy channels 9–67, which correspond to an energy range of about 3–20 keV, as specified by Serim et al. (2017). The data was barycentered using the FTOOL `faxbary`,

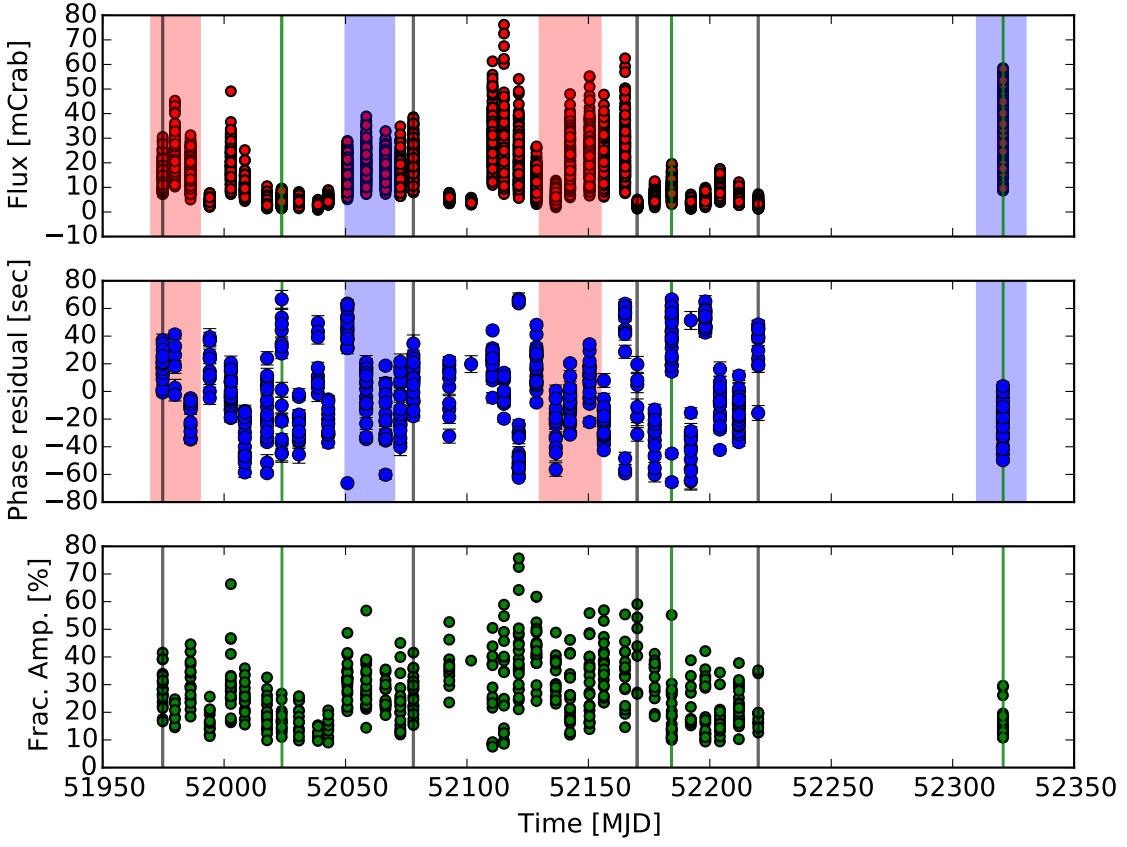

Figure 3.1: Top panel: The lightcurve for the *RXTE* data between March 6 to November 14 2001. Lower panel: The corresponding pulse phase. The red area marks the correlations between the flux and pulse phase, the blue area marks the anti-correlation and the green line marks the data segment that is zoomed in on in Fig. 3.2. The black lines mark the 4 times for which pulse profiles are shown in Fig. 3.3

Table 3.1: The parameters used in the epoch folding.

Parameter	Value
MJD	51974.7 - 52320.7
RA	17:32:02.16
DEC	-24:44:44.2
Epoch	51974.0
ν	0.007335526
$\dot{\nu}$	-2.0585$\times 10^{-12}$

using the JPL D405 Solar System coordinates and the source coordinates, from Cutri et al. (2003), RA: 17:32:02.16, DEC:-24:44:44.2. We then epoch folded the barycentered data in pulse profiles of 32 bins over the spin period, P_s=136.3228 s for segments of length $\sim$ 2000–3500s. We cross-correlated each pulsation with a sinusoid at the spin frequency and generated the time of arrivals (TOAs) for this data set. We selected only pulsations with a signal-to-noise (S/N) larger than 3.3 σ in order to achieve less than one false detection in our ensemble (composed by a total of $N = 538$ pulse profiles). The S/N is defined as the ratio between the pulse amplitude and its 1σ statistical error. The ephemeris used during the epoch folding are taken from Serim et al. (2017). To phase connect the data we used TEMPO2 version 2012.6.1.

3.3 Results

In the following sections we will go though the flux variations of GX 1+4 and compare these to variations in the pulse phase, in order to test if there is a correlation or anti-correlation. We look at both the full data set and three small segments of the data.

3.3.1 Phase connection

We have used archival data from *RXTE* approximately corresponding to the data segment labelled "*a*" in Serim et al. (2017), and we used the coherent timing solution from the same paper (see Table 3.1). We do this in order to reproduce their results and inspect the pulse phase residuals in order to later look for a pulse-phase correlation in the data. When folding the data we clearly detect pulsations with high S/N, but the pulse phase residuals are scattered between -0.5 and +0.5 pulse phase cycles, which means that the pulsations are not phase connected. We thus cannot recover the same results of Serim et al. (2017) with their proposed timing solution.

We thus consider the possibility that the true spin frequency (and derivatives) of GX 1+4 might be off with respect to the solution proposed by Serim et al. (2017) To look for a phase connected solution we thus keep all parameters fixed and vary the pulse frequency to explore the χ^2 surface and select the value that minimizes the χ^2. We used 1000 different pulse frequencies, varying between 0.0071355 Hz

and 0.0075355 Hz in steps of 4×10^{-7} Hz. The pulse frequency corresponding to the minimum χ^2 found still did not give a phase-connected solution. We then considered also variations of the pulse frequency derivative $\dot{\nu}$, exploring values between $-2.24585 \times 10^{-12}\,\mathrm{Hz\,s^{-1}}$ and $-1.6585\times10^{-12}\,\mathrm{Hz\,s^{-1}}$ in steps of $8 \times 10^{-16}\,\mathrm{Hz\,s^{-1}}$ and again we were unable to find a phase-connected solution. To further investigate the reason of this, we considered also the presence of a $\ddot{\nu}$, since Serim et al. (2017) provide also a measured value for that parameter. However we found no improvement in our attempt to phase connect the data. This is not surprising since the contribution of $\ddot{\nu}$ to the pulse phase variation with time can be considered negligible when compared to ν and $\dot{\nu}$. A difference between our analysis and that of Serim et al. (2017) is that our dataset spans a time range slightly larger than theirs, by about 2 months. However, again this makes no difference with regards to the final solution since the phase connections is not achieved in any segment of the data. We do see pulsations with high signal to noise throughout the observations, which means that the solution is sufficiently accurate to fold the data. An example of the pulse phase residuals found when using for example the solution given in Table 3.1 is given in Fig. 3.1.

Finally, since we are using only the fundamental frequency for our coherent timing analysis, we tested the presence of a 2^{nd} and 3^{rd} harmonic in the pulse profiles. Both were present in the data with relatively high significance (S/N up to ~ 15). However, they did not behave differently from the 1^{st} harmonic (i.e., the fundamental), and no phase connected solution could be found in this case.

3.3.2 Phase - Flux correlation

Another way to search for a phase connected solution is to try to maximize the strength of the phase–flux correlation, which has been observed so far in several accreting millisecond pulsars (for a more detailed discussion of this method see for example Patruno 2010). We thus tested whether there are similarities in the variations of the flux with the pulse phase residuals as seen in Patruno et al. (2009). To obtain the exact count rate we used only one PCU, namely PCU2, since this unit is always on during all observations. We use the count rate in this case because in this way we can create a lightcurve with the exact same time binning as the pulse phase time series. We then kept the Keplerian orbit fixed (see Table 1) and varied the pulse frequency and frequency derivative as explained in the previous section. We then fitted the data with the linear correlation

$$\phi = a + bF_x \tag{3.1}$$

where ϕ is the pulse phase, F_x is the X-ray count-rate and "a" and "b" are fitting parameters. We explored the χ^2 surface to find the value of ν that minimizes the χ^2 value. We explored a grid of 1000 values for ν and then fitted the phase residuals vs. flux with the linear relation in Eq. 3.1. We then found the minimum root-mean-squared (rms) value of the fit which gave us the best fit value of $\nu\sim$0.007417326 Hz. We re-folded the data with the new value for ν and iterated this entire procedure for a few times, but the minimum χ^2 value did not converge. This means that we are unable to find a global χ^2 minimum corresponding to a phase-connected

solution of the data. We then repeated the entire procedure by adding also the pulse frequency derivative $\dot{\nu}$ (and using again 1000 guess values) to verify whether the lack of a phase connection could be ascribed to a rapid variation of the pulse frequency over the time span of the observations. However, we could not find a global minimum for the χ^2 even in this case.

In summary, when using both standard χ^2 minimization methods with the pulse phases alone and when using the pulse-phase correlation method we cannot phase connect the solution. We stress, however, that pulsations were detected throughout the observations, which means that a coherent signal is present in the data, at least on a short timescale (of the order of a few rotational periods of the pulsar). The coherence of the signal is then lost when looking at longer (>hours) timescales. We then went back and used the TOA solution given in table 3.1 (Serim et al. 2017), and inspected the resulting light curves and pulse phase residuals, showing the minimum rms. These are shown in Fig. 3.1. The reason for this choice is that if the pulse phases keep their coherence on short timescales then it should still be possible to see correlations between flux and pulse phases on these timescales (assuming that such an effect exists in GX 1+4). From the figure it is clear that there is no simple long-term correlation or shape that is similar in the top two panels, but there are indeed a few segments of the top two panels on Fig. 3.1 where the flux and pulse phase residuals are correlated or anti-correlated. These are respectively marked in blue (anti-correlation) and red (correlation). The green lines on Fig. 3.1 are the three sections that are zoomed in on in Fig. 3.2, and the grey lines are the times where the pulse profiles are plotted, as seen in Fig. 3.3.

3.3.3 Short-term variability

Since we do see pulsations in every data point plotted in Fig. 3.1 this means that we recover part of the coherent signal with the solution used. On Fig. 3.2 the three data segments marked in green (in Fig. 3.1) are shown. The three segments were chosen due to the variations in the flux and phase residuals, where segment 1 has almost no variation in the flux but a large variation in the phase residuals, segment 2 has small variations in the flux with larger variations in the phase residuals but not as large as segment 1, and the 3rd segment has a variation in both flux and phase of somewhat similar order. On Fig. 3.2 the average of the phase residuals are corresponding to an overall slope of zero, indicating that the frequency is correctly measured. When looking at Fig. 3.2 it is evident that there is no clear correlation between the flux and phase residuals on a short time scale.

3.4 Discussion

3.4.1 Pulse Profiles

The TOA solution we have used throughout this chapter, found by Serim et al. (2017), was found using a template pulse profile. As reported earlier by Cui & Smith (2004), and as shown on Fig. 3.3 we see that the pulse profiles vary

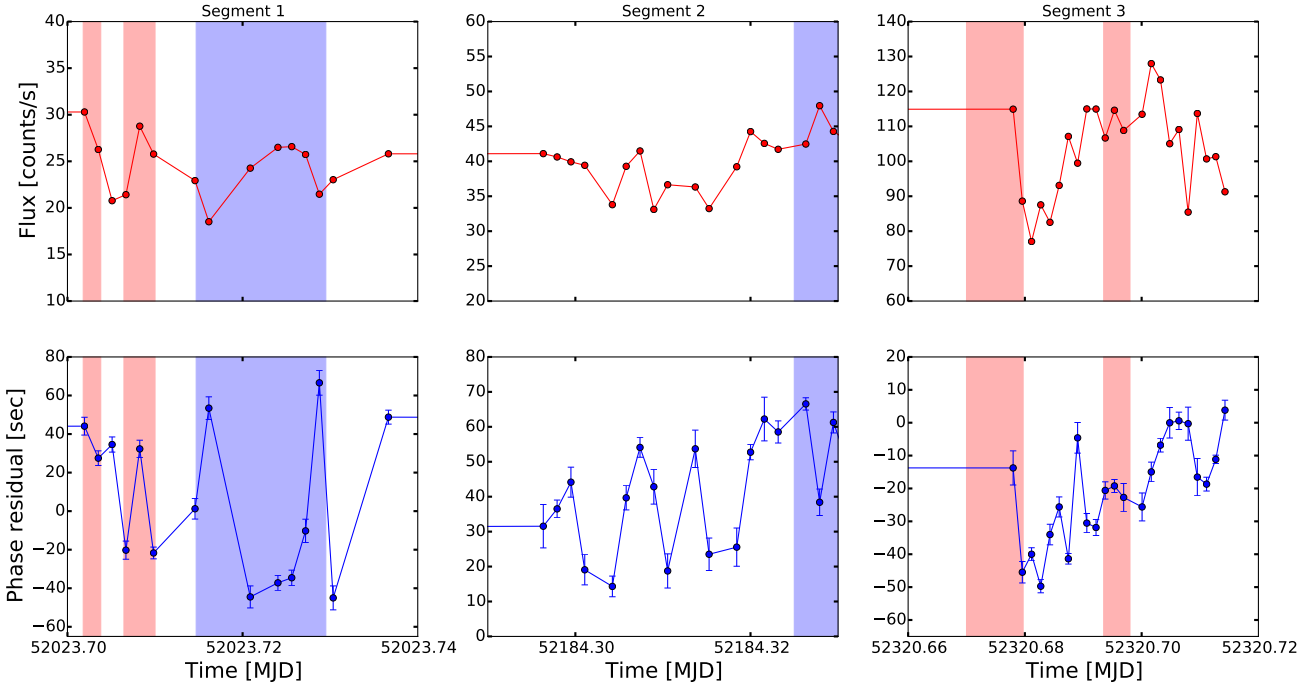

Figure 3.2: Top panel: Light curve of small data segment. Lower panel: Pulse Phase residuals for the same data segment. The data segment is marked on Fig. 3.1 in green. The red areas mark the correlations between pulse phase and flux and the blue are marks the anti-correlation between pulse phase and flux.

throughout the observation, so that it is not possible to use a single template high signal to noise pulse profile to perform the coherent timing analysis. Indeed, when the pulse shape variability is not properly taken into account there is the risk of introducing strong systematics in the results (Boynton et al. 1984; Hartman et al. 2008; Ibragimov & Poutanen 2009). We have, however, used the solution found by Serim et al. (2017) as our guess solution in order to find a phase connected solution of each harmonic separately (up to the 3rd harmonic), so to avoid the ambiguity in the definition of the pulse phase reference point. However, despite this precaution, we find that it is not possible to create a phase connected solution.

The pulse profiles seen on Fig. 3.3 show an example of the variability in the pulse shape.

3.4.2 Phase - Flux correlation – consequence for AMXPs

A proposed scenario for explaining the pulse phase and flux correlation in accreting millisecond pulsars was the movement of the hot spot, perhaps linked to movement of the magnetic field (Patruno et al. 2009). In this chapter and in the paper by Bak Nielsen et al. (2017) it has been tested if there is any such correlation in the pulsars with a higher magnetic field, which would possibly rule out movement of the hot spot. It is found in this chapter and in Bak Nielsen et al. (2017), concerning the LMXB pulsar 2A 1822-371, that it is not possible to find a phase - flux correlation. As described in section 3.3.2 in this chapter, it is also not possible to find any phase - flux correlation for GX 1+4. Because 2A 1822-371 and GX 1+4 are pulsars with a higher magnetic field than the AMXPs, it is possible that the pulse phase - flux correlation found in AMXPs (Patruno et al. 2009) is dependent on the magnetic field strength. If the magnetic field is strong enough this could prevent the movement of the hot spot on the neutron star surface, which was suggested to be a possible explanation for the phase - flux correlation (Patruno et al. 2009).

3.4.3 Short term flux variability

We can infer, from our attempts to phase connect the data, that the signal from GX 1+4 is not coherent over a time scale of days or longer. Furthermore, since we see short term variability in both the flux and the phase and we do not see a correlation between the flux and phase we infer that something is varying quickly on the neutron star surface. This is also supported by the change in the pulse profile shape. The variation could for example be the shape of the hot spot or perhaps the geometry of the beam. We observe pulsations throughout the observations, which does imply that even though we are not able to find a phase connected solution, we keep the coherence of the signal on a time scale of hours.

From the above, we would infer, that wind accretion is quite likely. The wind would attach to random field lines and thus create short term variability, pulse shape variability and make it impossible to find a phase coherent (long-term) solution (González-Galán et al. 2012; van den Eijnden et al. 2018). The short-term variability is similar to variability seen in Vela X-1, a HMXB, that accretes

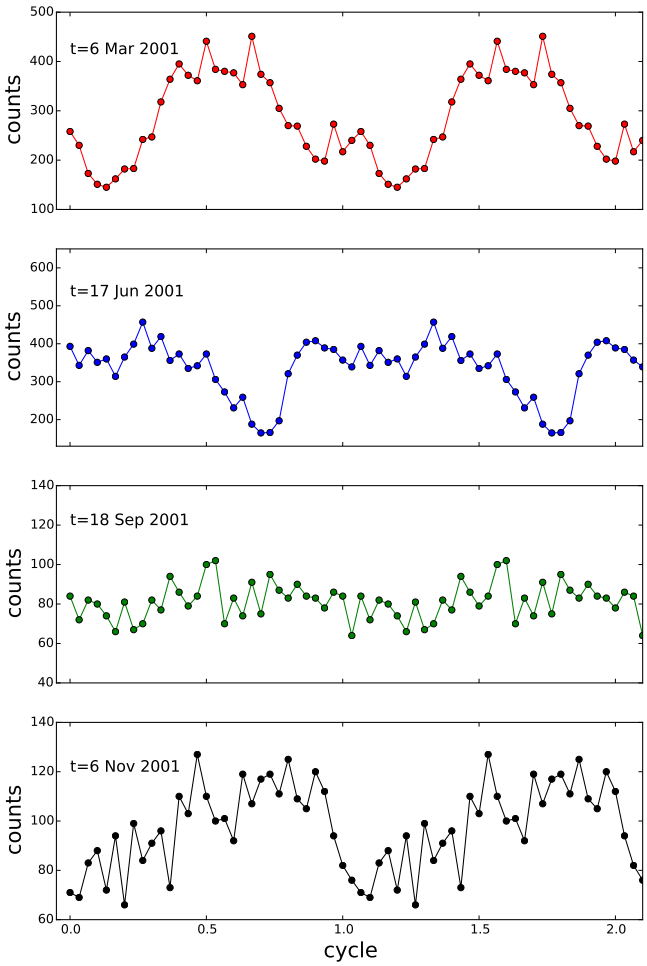

Figure 3.3: Four pulse profiles at different times. The first and last pulse profile in the Figure correspond to the initial and final epoch of the folded data. The two middle panels correspond to in-between times (marked in each panel).

through wind accretion (Boynton et al. 1986; Malacaria et al. 2016). However, it should be noted, that it is, at least on short timescales, possible to create coherent timing solutions to Vela X-1 (Nagase 1989). Due to the short-term variations, wind accretion seems to be the most likely accretion mechanism of GX 1+4, considering the variability on short time scales.

3.5 Conclusions

We examined about a year of *RXTE* data of GX 1+4, from March 2001 to February 2002. We conclude that it is not possible to phase connect the data due to the nature of the accretion process, which most likely proceeds via wind from the giant donor companion in the binary. We tested if a pulse phase - flux correlation was present in the data, similar to what is sometimes seen in the AMXPs and find that such a correlation does not appear to be present in GX 1+4. This might be due to the stronger magnetic field of the pulsar or, alternatively, to the different nature of the accretion process, which, in AMXPs, proceeds via an accretion disk interacting with the pulsar magnetosphere. The findings of this chapter, along with the findings of Bak Nielsen et al. (2017) does suggest that the phase - flux correlation is only present for pulsars with low magnetic fields of the order 10^8-10^9 G, as is the case for the AMXP. In this chapter we further suggest that there are some similarities between GX 1+4 and HMXBs such as for example VELA X-1, they both show variations in the pulse profile which is suggested to originate from wind accretion.

Bibliography

Bak Nielsen A.-S., Patruno A., D'Angelo C., 2017, MNRAS, 468, 824
Boynton P. E., Deeter J. E., Lamb F. K., Zylstra G., Pravdo S. H., White N. E., Wood K. S., Yentis D. J., 1984, ApJ, 283, L53
Boynton P. E., Deeter J. E., Lamb F. K., Zylstra G., 1986, ApJ, 307, 545
Chakrabarty D., et al., 1997, ApJ, 481, L101
Cui W., Smith B., 2004, ApJ, 602, 320
Cutler E. P., Dennis B. R., Dolan J. F., 1986, ApJ, 300, 551
Cutri R. M., et al., 2003, VizieR Online Data Catalog, 2246
Davidsen A., Malina R., Bowyer S., 1977, ApJ, 211, 866
Dotani T., Kii T., Nagase F., Makishima K., Ohashi T., Sakao T., Koyama K., Tuohy I. R., 1989, PASJ, 41, 427
González-Galán A., Kuulkers E., Kretschmar P., Larsson S., Postnov K., Kochetkova A., Finger M. H., 2012, A&A, 537, A66
Hartman J. M., et al., 2008, ApJ, 675, 1468
Hinkle K. H., Fekel F. C., Joyce R. R., Wood P. R., Smith V. V., Lebzelter T., 2006, ApJ, 641, 479
Ibragimov A., Poutanen J., 2009, MNRAS, 400, 492
Ιłkiewicz K., Mikołajewska J., Monard B., 2017, A&A, 601, A105
Jahoda K., Markwardt C. B., Radeva Y., Rots A. H., Stark M. J., Swank J. H., Strohmayer T. E., Zhang W., 2006, ApJS, 163, 401
Lewin W. H. G., Ricker G. R., McClintock J. E., 1971, ApJ, 169, L17
Malacaria C., Mihara T., Santangelo A., Makishima K., Matsuoka M., Morii M., Sugizaki M., 2016, A&A, 588, A100
Mony B., et al., 1991, A&A, 247, 405
Nagase F., 1989, PASJ, 41, 1
Patruno A., 2010, ApJ, 722, 909
Patruno A., Watts A. L., 2012, preprint, (`arXiv:1206.2727`)
Patruno A., Wijnands R., van der Klis M., 2009, ApJ, 698, L60
Patruno A., Alpar M. A., van der Klis M., van den Heuvel E. P. J., 2012, ApJ, 752, 33
Pereira M. G., Braga J., Jablonski F., 1999, ApJ, 526, L105
Rea N., Stella L., Israel G. L., Matt G., Zane S., Segreto A., Oosterbroek T., Orlandini M., 2005, MNRAS, 364, 1229
Serim M. M., Şahiner Ş., ćerri-Serim D., Inam S. ć., Baykal A., 2017, MNRAS, 469, 2509
Yoshida Y., Kitamoto S., Suzuki H., Hoshino A., Naik S., Jaisawal G. K., 2017, ApJ, 838, 30
van Straaten S., van der Klis M., Méndez M., 2003, ApJ, 596, 1155
van den Eijnden J., Degenaar N., Russell T. D., Miller-Jones J. C. A., Wijnands R., Miller J. M., King A. L., Rupen M. P., 2018, MNRAS, 474, L91